Oxygen transport and incorporation mechanisms in the dry thermal oxidation of 6H-SiC

C. Radtke, I. J. R. Baumvol, B. C. Ferrera, and F. C. Stedile

Citation: Applied Physics Letters **85**, 3402 (2004); doi: 10.1063/1.1807033
View online: http://dx.doi.org/10.1063/1.1807033
View Table of Contents: http://scitation.aip.org/content/aip/journal/apl/85/16?ver=pdfcov
Published by the AIP Publishing

Oxygen transport and incorporation mechanisms in the dry thermal oxidation of 6H-SiC

C. Radtke
Commissariat à l'Energie Atomique, DSM-DRECAM-SPCSI-SIMA, Bâtiment 462, Saclay, 91191 Gif sur Yvette Cedex, France

I. J. R. Baumvol
Centro de Ciências Exatas e Tecnológicas-UCS, Av. Francisco G. Vargas 1130, 95070-560, Caxias do Sul, RS, Brazil

B. C. Ferrera and F. C. Stedile[a)]
Instituto de Química, UFRGS, Avenida Bento Gonçalves 9500, 91509-900, Porto Alegre, RS, Brazil

(Received 26 April 2004; accepted 17 August 2004)

Thermal oxidation of 6H-SiC was investigated by means of isotopic tracing and narrow nuclear resonant reaction profiling techniques. The mechanisms of oxygen transport and incorporation were accessed by sequential oxidations in dry O_2 enriched or not in the ^{18}O isotope and subsequent determinations of the ^{18}O profiles. After sequential $^{16}O_2/^{18}O_2$ or $^{18}O_2/^{16}O_2$ oxidations of SiC, the ^{18}O profiles were seen to be markedly different from those observed in Si oxidation, which led to the identification of different mechanisms of oxygen incorporation and transport. The gradual nature of the SiO_2/SiC interface was also evidenced by the ^{18}O depth distributions in samples oxidized in a single step in ^{18}O-enriched O_2. A probable explanation for this gradual SiO_2/SiC interface is shown to be the formation of C clusters during oxidation. © *2004 American Institute of Physics*. [DOI: 10.1063/1.1807033]

SiC is a wide band gap semiconductor material, possessing desirable properties for devices operating in high temperature, high frequency, high power and/or high voltage conditions. Furthermore, SiC is the only compound semiconductor that can be thermally oxidized forming a film of SiO_2, an outstanding dielectric material for device applications. Despite all these advantages, the electrical characteristics of devices built on SiC are worse than those prepared on Si, mainly as a result of the detrimental properties of the formed SiO_2/SiC interface.[1] This fact hampers the wide utilization of this semiconductor in the fabrication of power devices. Aimed at improving the properties of the SiO_2/SiC interface, different ways of growing the SiO_2 layer[2,3] and different post-oxidation treatments[4–7] have already been proposed. In order to achieve further improvement, fundamental knowledge of the mechanisms involved in thermal oxidation of SiC and the effects of each oxidation parameter (temperature, gas pressure, etc.) are of major importance. This knowledge will make it possible to modify conveniently the oxidation process and improve the electrical characteristics of the final device.

The structure and composition of the transition layer between SiO_2 and SiC is still not as well understood as the SiO_2/Si interface. The fundamental difference between these systems is the presence of C in the former. Investigations of thermal oxide growth on SiC indicate that, in the surface and bulk regions, the oxide is similar to that grown on Si,[1,8–10] whereas incompletely oxidized C and/or Si are found near the interface.[1,3,11–13] Besides, the oxidation of SiC entails the production of carbonaceous species (mainly CO) that diffuse through the oxide layer, giving rise to a new branch of possible reactions.

In the present work we investigate the atomic transport and incorporation of oxygen during thermal oxidation of SiC, with special attention to the oxide/SiC transition region. These results are compared to those of similarly prepared Si samples, whose oxidation mechanisms are well established. The experiments consisted essentially of the sequential thermal growth of oxides in natural $O_2(^{16}O_2)$ and in 97% ^{18}O-enriched $O_2(^{18}O_2)$, alternating the gas sequence, or performing oxidations only in $^{18}O_2$.

6H-SiC and Si (001) wafers were cleaned in a standard RCA routine, followed by a dip for 30 s in a 5% HF aqueous solution, aimed at removing the native oxide, and water rinsing for 30 s. All oxides were grown in a resistively heated quartz tube furnace under a static pressure of 100 mbar. ^{18}O profiles were determined by narrow nuclear resonant reaction profiling (NRP) using the resonance at 151 keV in the cross-section curve of the $^{18}O(p,\alpha)^{15}N$ nuclear reaction. Profiles and excitation curves were normalized by the areal densities determined by nuclear reaction analysis and Rutherford backscattering spectrometry in channeling geometry.[14]

Figure 1(a) shows the excitation curves and the corresponding ^{18}O depth distributions in samples oxidized in two steps: $^{16}O_2$ at 1100 °C followed by $^{18}O_2$. The profile obtained for the SiO_2/Si structure (dotted line) presents the well-known ^{18}O-rich regions: erfc-like at the sample surface and box-like in the oxide/Si interface region.[14] In the bulk of the oxide, the absence of ^{18}O in concentrations above its natural abundance (0.2%) indicates that $^{18}O_2$ molecules in the second oxidation step diffuse through the already formed ^{16}O-oxide without interacting with it, reacting with Si at an abrupt interface to form new $Si^{18}O_2$.[15] The same sequential oxidations were performed on the Si face of the SiC wafers (SiC (0001)). The ^{18}O profile in the sample reoxidized in $^{18}O_2$ at 950 °C (dash-dotted line) in the surface region is

a)Electronic mail: fernanda@iq.ufrgs.br

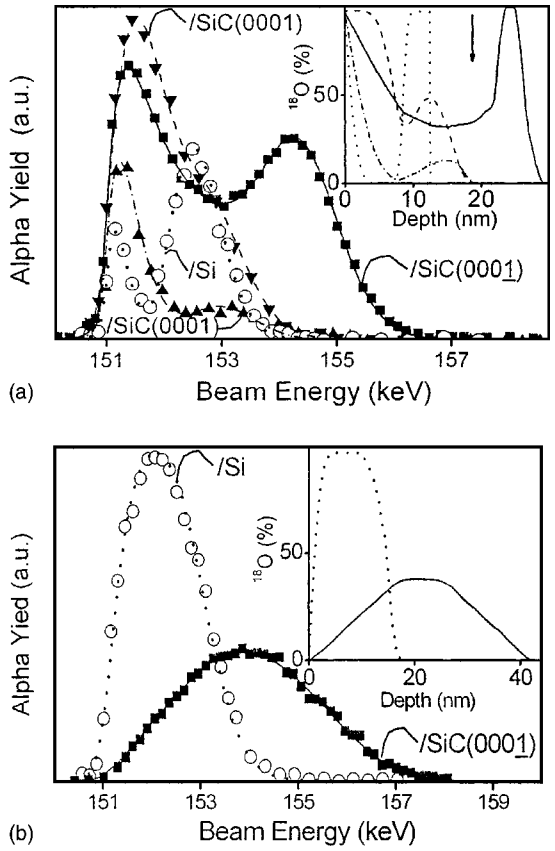

FIG. 1. Experimental excitation curves (symbols) of the $^{18}O(p,\alpha)^{15}N$ nuclear reaction and the corresponding simulations (lines) for silicon oxide films thermally grown on Si (001) (circles), SiC (0001) (triangles), and SiC (000$\underline{1}$) (squares). The type of oxidized substrate is indicated. (a) Samples were first oxidized at 1100 °C in $^{16}O_2$ and then reoxidized in $^{18}O_2$ at 950 °C (circles and up triangles) or 1100 °C (squares and down triangles). The position of the SiO_2/SiC interface after the first oxidation step of the SiC (0001) sample reoxidized at 950 °C (dash-dotted line) is indicated by an arrow. (b) Samples were first oxidized at 1100 °C in $^{18}O_2$ and then reoxidized in $^{16}O_2$ at 950 °C (circles) and 1100 °C (squares). ^{18}O profiles used for the simulations of excitation curves are shown in the respective insets with the same type of line of the respective simulations. ^{18}O concentration is normalized to O in stoichiometric SiO_2. a.u. stands for arbitrary units.

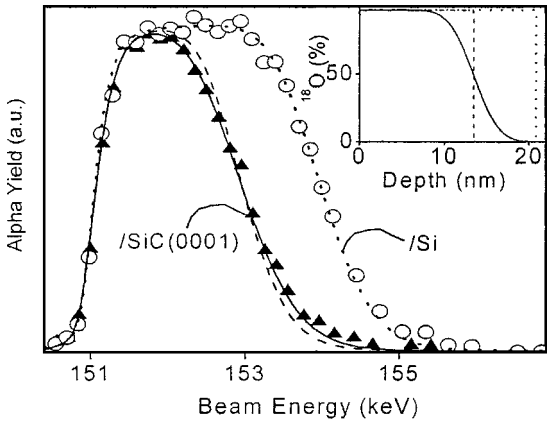

FIG. 2. Experimental excitation curves (symbols) of the $^{18}O(p,\alpha)^{15}N$ nuclear reaction and the corresponding simulations (lines) for silicon oxide films thermally grown on SiC (0001) (triangles) and on Si (001) (circles). The type of oxidized substrate is indicated. Oxidations were performed in $^{18}O_2$ at 1100 °C. ^{18}O profiles used for the simulations of excitation curves are shown in the inset with the same type of line of the respective simulations. ^{18}O concentration is normalized to O in stoichiometric SiO_2. a.u. stands for arbitrary units.

erfc-like as in the case of Si. However, ^{18}O is also incorporated in the bulk of the oxide and in the interface region, where its concentration is only 13% and not equal to the isotopic labeling of the gas (97%) as in the case of Si substrate. The position of the oxide/SiC interface in this sample, after the first oxidation step, is indicated by an arrow in Fig. 1(a). After the second oxidation, in $^{18}O_2$, the final thickness remains roughly the same. The ^{18}O profile in the SiC (0001) sample oxidized in the second step in $^{18}O_2$ at 1100 °C (dashed line) is also shown. The SiO_2 layer grown in the first oxidation step was not sufficiently thick to clearly separate the surface and interface contributions of ^{18}O. Besides, the amount of ^{18}O corresponding to the estimated interfacial peak is too small to allow for a study on how ^{18}O incorporates close to the SiO_2/SiC interface. Thus, the oxidation of the SiC (000$\underline{1}$) (or C face) was undertaken, because it has a higher oxidation rate, resembling more the Si oxidation rate than the one of SiC (0001). It enables the incorporation of higher amounts of ^{18}O in the interfacial region in reasonable oxidation times. The ^{18}O depth distribution of this sample is also shown (solid line). The ^{18}O interfacial peak in the case of the oxidized C face of the SiC sample evidences an ^{18}O concentration that varies gradually at both sides of a narrow plateau of stoichiometric $Si^{18}O_2$ instead of the abrupt $Si^{16}O_2/Si^{18}O_2$ transition observed in the case of Si. Besides, ^{18}O is also found in the bulk of the oxide film.

Figure 1(b) shows the ^{18}O profiles in Si and SiC (000$\underline{1}$) samples oxidized in the same way as the precedent ones but alternating the gas sequence: first oxidation in $^{18}O_2$ followed by $^{16}O_2$. ^{18}O is seen to occupy the sites analogous to those occupied by ^{16}O atoms in Fig. 1(a) and vice versa. In the case of the Si oxidized sample [dotted line in Fig. 1(b)], there is a rather abrupt transition between the bulk ^{18}O-rich oxide and the near-interface ^{16}O-oxide, evidencing that the first formed $Si^{18}O_2$ layer remained approximately unaltered after the second oxidation step. However, the ^{18}O profile obtained from the SiC oxidized sample is strikingly different in all film regions [solid line in Fig. 1(b)], evidencing an ^{18}O concentration in the bulk region much lower than the isotopic labeling of the $^{18}O_2$ gas, as well as the presence of a substantial amount of ^{18}O in the near-interface region, with a gradual transition between these two regions.

Figure 2 shows the ^{18}O profiles obtained from the SiC and Si samples oxidized in a single step in $^{18}O_2$. An abrupt interface between SiO_2 and Si is observed (dotted line). However, in the case of the oxide/SiC interface the same box-like distribution (dashed line) did not lead to a satisfactory agreement between experimental data and the simulation curve. A good fit is only obtained if one assumes a graded interface (solid line). The gradual decrease of the ^{18}O concentration near the SiO_2/SiC interface brings about the discussion on how the structure and/or composition of this interface as well as the reaction-diffusion phenomena involved in the oxidation of SiC could give rise to such a gradual transition. One could attribute it to interface roughness. However, this hypothesis was ruled out by high resolution TEM images.[12] Alternatively, the presence of another element can lower the local O-concentration. Since the existence of a C-rich region close to the SiO_2/SiC interface was shown by electron energy loss spectroscopy analysis,[12] one may admit that the presence of C locally depletes the oxygen concentration and one observes the nonabrupt oxide/SiC in-

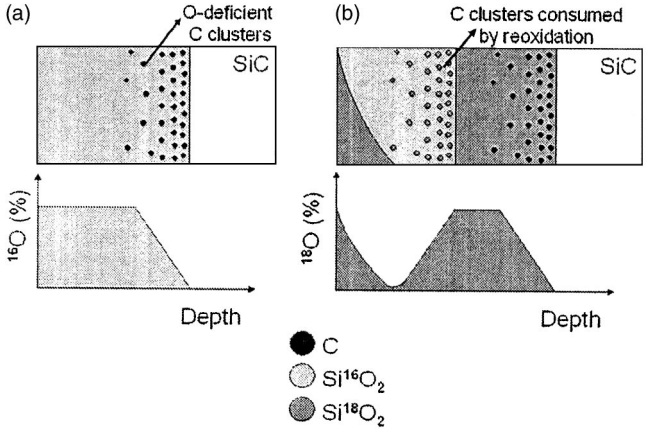

FIG. 3. Representation of a SiC sample submitted to sequential oxidations at high temperature: (a) after a first oxidation in $^{16}O_2$ and (b) after further oxidation in $^{18}O_2$. The resulting ^{16}O and ^{18}O profiles are represented, respectively.

terface as shown in Fig. 2. This phenomenon also leads to the different ^{18}O distributions observed in SiC samples as compared to those of Si in the interface region. In the case of Si, there is no measurable mixture of oxygen incorporated in distinct oxidation steps, except for the oxide surface. In the case of SiC, the results shown in Fig. 1 evidence a mixture of ^{16}O and ^{18}O from different oxidation steps also in the SiO_2/SiC transition region. We propose that this mixture is intervened by the formation and consumption of C clusters during oxidation as represented pictorially in Fig. 3.

Following this reasoning, CO molecules produced in the near-interface region by reaction of O_2 with SiC will diffuse and may undergo further chemical reactions. Possible reactions of CO with the SiO_2 network were investigated and nucleation and growth of C clusters in the oxide film and the emission of CO_2 molecules was theoretically predicted.[16] They also showed that these clusters can be consumed by their reaction with diffusing O_2 molecules during oxidation. Thus, in the oxidation process, there is simultaneous formation of C clusters and their progressive consumption by reaction with O_2, resulting in a depth distribution of C clusters that can be like the one shown in Fig. 3(a). The resulting oxygen profile is analogous to the solid line one in Fig. 2, obtained by oxidizing SiC in a single step. A second oxidation step in $^{18}O_2$ following a first step in $^{16}O_2$ will cause ^{18}O incorporation by: (i) the formation of new $Si^{18}O_2$ at the interface, (ii) the consumption of the carbon clusters, and (iii) isotopic exchange in the surface region. Mechanism (ii) is confirmed by the ^{18}O profile of the SiC sample oxidized first at 1100 °C in $^{16}O_2$ followed by oxidation at 950 °C in $^{18}O_2$ [dash-dotted line in Fig. 1(a)]. In this case, during the second, lower temperature oxidation step, the CO production is strongly diminished and, consequently, many less C clusters are formed. Therefore, ^{18}O incorporation is mostly a result of consumption of the C clusters already formed in the previously existing oxide layer. In fact, it is known that a low temperature reoxidation of the SiO_2/SiC structure is responsible for a decrease in the density of electronic states of the SiO_2/SiC interface, related to a reduction on the concentration of carbonaceous species.[7] Performing a reoxidation (in $^{18}O_2$) at a higher temperature leads to, besides the consumption of the previously formed clusters, oxidation of the SiC substrate, creating a new layer of $Si^{18}O_2$ and forming new C clusters close to the new SiO_2/SiC interface. The near-interface ^{18}O distribution that emerges from this model is represented in Fig. 3(b). The solid line profile in Fig. 1(a), from an oxidized SiC (000$\underline{1}$) sample, corroborates this idea.

A further test to the validity of this reasoning could be obtained by performing a low temperature reoxidation in $^{18}O_2$ of the SiC sample of Fig. 2. If the preceding model is valid, this procedure should transform the smooth decrease of the ^{18}O concentration observed before the reoxidation step to a more abrupt transition. In fact, this confirmation was achieved[17] using x-ray photoelectron spectroscopy to observe the effect of a low temperature reoxidation in an effort to obtain a more abrupt SiO_2/SiC interface. Nevertheless, we do not exclude the existence of other possible mechanisms that can contribute to the incorporation of ^{18}O in the already formed $Si^{16}O_2$ layer, like the ejection of Si interstitials from the substrate and $^{16}O-{}^{18}O$ isotopic exchange.[18]

In summary, based on the present findings this letter has identified different mechanisms through which oxygen is incorporated in the bulk and interface oxide regions during thermal oxidation of SiC, namely consumption of carbon clusters and reaction with the SiC substrate in a wider region as compared to Si oxidation. The dynamics of these processes gives rise to different ^{18}O profiles. However, the present findings do not exclude the existence of other mechanisms that can also contribute to the final ^{18}O depth distributions. The abruptness of the SiO_2/SiC interface was also investigated, evidencing that the formation of C clusters during oxidation is a probable explanation for the gradual nature of this interface. In order to get further insight into this subject, we intend to perform C depth profiling of these samples with secondary ion mass spectrometry and NRP techniques.

[1] V. V. Afanas'ev, M. Bassler, G. Pensl, and A. Stesmans, Mater. Sci. Forum **389–393**, 961 (2002).
[2] G. Lucovsky, H. Niimi, A. Golz, and H. Kurz, Appl. Surf. Sci. **123**, 435 (1998).
[3] F. Amy, P. Soukiassian, Y. K. Hwu, and C. Brylinski, Phys. Rev. B **65**, 165323 (2002).
[4] G. Chung, C.C. Tin, J.R. Williams, K. McDonald, M. Di Ventra, R.K. Chanana, S. T.Pantelides, L.C. Feldman, and R.A. Weller, Appl. Phys. Lett. **77**, 3601 (2000).
[5] R. Schorner, P. Friedrichs, D. Peters, D. Stephani, S. Dimitrijev, and P. Jamet, Appl. Phys. Lett. **80**, 4253 (2002).
[6] K. Y. Cheong, S. Dimitrijev, J.S. Han, and H.B. Harrison, J. Appl. Phys. **93**, 5682 (2003).
[7] A. Ekoué, O. Renault, T. Billon, L. Di Cioccio, and G. Guillot, Mater. Sci. Forum **433–436**, 555 (2003).
[8] M. B. Johnson, M. E. Zvanut, and O. Richardson, J. Electron. Mater. **29**, 368 (2000).
[9] K. McDonald, M. B. Huang, R. A. Weller, L. C. Feldman, J. R. Williams, F.C. Stedile, I. J. R. Baumvol, and C. Radtke, Appl. Phys. Lett. **76**, 568 (2000).
[10] I.C. Vickridge, I. Trimaille, J.-J. Ganem, S. Rigo, C. Radtke, I.J.R. Baumvol, and F.C. Stedile, Phys. Rev. Lett. **89**, 256102 (2002).
[11] C. Virojanadara and L.I. Johansson, Surf. Sci. **472**, L145 (2001).
[12] K.C. Chang, N.T. Nuhfer, L.M. Porter, and Q. Wahab, Appl. Phys. Lett. **77**, 2186 (2000).
[13] C. Radtke, I. J. R. Baumvol, J. Morais, and F. C. Stedile, Appl. Phys. Lett. **78**, 3601 (2001).
[14] I. J. R. Baumvol, Surf. Sci. Rep. **36**, 1 (1999).
[15] B.E. Deal and A.S. Grove, J. Appl. Phys. **36**, 3770 (1965).
[16] S. Wang, M. Di Ventra, S.G. Kim, and S.T. Pantelides, Phys. Rev. Lett. **86**, 5946 (2001).
[17] G.G. Jernigan, R. E. Stahlbush, and N. S. Saks, Appl. Phys. Lett. **77**, 1437 (2000).
[18] I. Trimaille, J.-J. Ganem, I.C. Vickridge, S. Rigo, G. Battistig, E. Szilagyi, I.J.R. Baumvol, C. Radtke, and F.C. Stedile, Nucl. Instrum. Methods Phys. Res. B **219**, 914 (2004).